

# Co<sub>3</sub>O<sub>4</sub> based catalysts for NO oxidation and NO<sub>x</sub> reduction in fast SCR process

Muhammad Faisal Irfan, Jeong Hoi Goo, Sang Done Kim <sup>\*</sup>

*Department of Chemical and Biomolecular Engineering, Energy and Environmental Research Center,  
Korea Advanced Institute of Science and Technology (KAIST), 373-1 Gusong-dong,  
Yuseong-gu 305-701, Daejeon, Republic of Korea*

Received 3 May 2007; received in revised form 21 September 2007; accepted 23 September 2007  
Available online 29 September 2007

## Abstract

Reaction activities of several developed catalysts for NO oxidation and NO<sub>x</sub> (NO + NO<sub>2</sub>) reduction have been determined in a fixed bed differential reactor. Among all the catalysts tested, Co<sub>3</sub>O<sub>4</sub> based catalysts are the most active ones for both NO oxidation and NO<sub>x</sub> reduction reactions even at high space velocity (SV) and low temperature in the fast selective catalytic reduction (SCR) process. Over Co<sub>3</sub>O<sub>4</sub> catalyst, the effects of calcination temperatures, SO<sub>2</sub> concentration, optimum SV for 50% conversion of NO to NO<sub>2</sub> were determined. Also, Co<sub>3</sub>O<sub>4</sub> based catalysts (Co<sub>3</sub>O<sub>4</sub>-WO<sub>3</sub>) exhibit significantly higher conversion than all the developed DeNO<sub>x</sub> catalysts (supported/unsupported) having maximum conversion of NO<sub>x</sub> even at lower temperature and higher SV since the mixed oxide Co-W nanocomposite is formed. In case of the fast SCR, N<sub>2</sub>O formation over Co<sub>3</sub>O<sub>4</sub>-WO<sub>3</sub> catalyst is far less than that over the other catalysts but the standard SCR produces high concentration of N<sub>2</sub>O over all the catalysts. The effect of SO<sub>2</sub> concentration on NO<sub>x</sub> reduction is found to be almost negligible may be due to the presence of WO<sub>3</sub> that resists SO<sub>2</sub> oxidation.

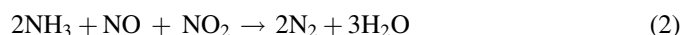
© 2007 Elsevier B.V. All rights reserved.

**Keywords:** Fast SCR; NO<sub>x</sub> removal; Co<sub>3</sub>O<sub>4</sub>; NO oxidation; Catalyst

## 1. Introduction

Exhaust gases from stationary and mobile combustion sources contain nitrogen oxides (NO, NO<sub>2</sub> and N<sub>2</sub>O) that contribute to photochemical smog, acid rain, ozone depletion and the green house effects. Removal of these contaminants in compliance with the environmental emission standard is necessary and various wet and dry processes have been developed. In the past, most research works have been focused on the standard SCR process to remove nitrogen oxides by ammonia since NO<sub>x</sub> formed in combustion processes is typically composed of >90% NO. Recently, a newly designed process namely, the fast SCR process has been developed that has faster reaction rate (almost 10 times) and high NO<sub>x</sub> removal efficiency than the standard SCR [1]. The high DeNO<sub>x</sub> conversion rate in the fast SCR process can be achieved by using an oxidation catalyst at upstream of the SCR unit so as to

convert *ca.* 50% of NO to NO<sub>2</sub> and this indirectly enables to reduce the SCR catalyst volume. In fast SCR process, two main reactions contribute to NO<sub>x</sub> conversion by ammonia:



For NO oxidation, several different catalysts have been reported in which the Pt based catalysts are found to be the most active one [2–4]. Recently, some metal oxide catalysts without support like MnO<sub>x</sub>, CuO<sub>x</sub>, etc. have also been investigated for NO oxidation but the conversion has been found to be unsatisfactory [5,6]. Similarly, for the standard SCR of NO, a great variety of different catalysts (supported/unsupported) such as MnO<sub>x</sub>/Al<sub>2</sub>O<sub>3</sub>, MnO<sub>x</sub>, Fe-Mn or Mn-Ce mixed oxides and commercial catalysts like V<sub>2</sub>O<sub>5</sub>/TiO<sub>2</sub> promoted by WO<sub>3</sub> and/or MoO<sub>3</sub> catalysts have been reported but these commercial type catalysts found to be suitable for application in a relatively narrow temperature window 300–400 °C [7–12]. Recently, this commercial catalyst has been tested for the fast SCR and found that it provides appropriate DeNO<sub>x</sub> conversion

<sup>\*</sup> Corresponding author. Tel.: +82 42 869 3953; fax: +82 42 869 3910.

E-mail address: [kimsd@kaist.ac.kr](mailto:kimsd@kaist.ac.kr) (S.D. Kim).

at relatively low-temperature window (250–300 °C) [1]. Hence, there is still a need for special low-temperature SCR catalysts since  $V_2O_5/WO_3-TiO_2$  has its optimum at the intermediate temperature. It is still good at the low-temperature end, but there are better formulations with a pronounced low-temperature optimum.

In the present study, the reaction activities of different catalysts prepared by the precipitation method (PM) and the incipient wetness impregnation method (IM) for NO oxidation and  $NO_x$  reduction were determined in a fixed bed reactor. Also, the effects of calcination temperatures, optimum SV for 50% conversion of NO to  $NO_2$ ,  $SO_2$  concentration and the formation of  $N_2O$  over  $Co_3O_4$  based catalysts on NO oxidation and  $NO_x$  reduction were determined.

## 2. Experimental

The identified catalysts were subsequently prepared for the fast SCR process, include (i) supported and unsupported oxides of Co, Cu, Mn and Ce, (ii) Co-Mn, Ce-Mn and Co-W mixed oxides and (iii) low Pt loaded (0.5 wt%) catalysts, only for NO oxidation, with the added  $WO_3$ ,  $V_2O_5$  for suppression of  $SO_2$  oxidation.

### 2.1. Catalyst preparation

The supported catalysts typically having a metal loadings of 20 wt% that were prepared by the IM employing weakly sulphating supports ( $TiO_2$ , Millennium chemicals;  $SiO_2$ , Aldrich Co.). All the impregnated metals such as Pt, W and V were obtained from their compounds like tetraammineplatinum(II) chloride hydrate, ammonium metatungstate hydrate and ammonium metavanadate, respectively, which were supplied by Aldrich Co. For all the samples, 2.5 g of the support material was used. The impregnated materials were added on the support, and then homogenized them for 1 h. Other unsupported metal oxides and mixed oxides were prepared by the PM using excess ammonia solution as a precipitator except Co-W mixed oxide which was produced by IM.  $Co_3O_4$  was prepared by PM from its nitrate solution and then  $WO_3$  was loaded over it by IM. In the PM, all the materials were used in nitrate form (Aldrich Co.) such as cobalt nitrate, manganese nitrate, cerium nitrate and copper nitrate. All the nitrate solutions were prepared of 1 M except ammonia solution which was prepared by 0.1 M in order to maintain pH of nearly 10. All solutions were prepared at room temperature. After adding ammonia solution, the precipitates were formed that were washed with distilled water and aged them for 1 h. All catalysts prepared by both the IM and PM were then dried at 120 °C for 4 h and then calcined at 350 °C except Pt based catalysts which were calcined at 500 °C as Pt oxides ( $PtO$ ,  $PtO_2$ ) are formed which are stable at 350–425 °C. The sizes of all the powder catalysts were ranged from –50 to +60 meshes. The resulting materials were characterized by using the nitrogen physisorption (BET surface area) and X-ray diffraction (XRD) analyses.

### 2.2. Catalytic tests

The activity of these catalysts for the fast SCR process was measured in a fixed bed quartz reactor (8 mm I.D.). The experimental equipment consists of three sections: reactor, gas feeding system and gas analyzer. The catalyst powders were loaded with an aid of quartz wool and heated to the desired reaction temperature by IR heater with PID controllers. The gas flow rates were regulated by mass flow controllers (MKS 1179) and the total gas flow rate was 1500 cc/min. Water was dosed into  $N_2$  and  $O_2$  gas stream by passing through a water saturator at 52 °C. All the gas lines were heated to 180 °C to prevent formation and deposition of ammonium nitrate and ammonium sulphate. Concentrations of NO,  $NO_2$ ,  $SO_2$  and  $O_2$  were continuously measured by non-dispersive infrared analyzer (NDIR) type gas analyzers (Fuji Electric Instruments Co., ZKJ-2). These two reactions, NO oxidation and  $NO_x$  reduction, were performed separately in the same experimental setup but during the  $NO_x$  reduction reaction, an ammonia trap containing 4% boric acid solution was installed at the upstream of gas analyzer in order to avoid errors caused by un-reacted ammonia. Concentrations of  $N_2O$  and  $NH_3$  were measured by NDIR gas analyzer (Hartmann & Braun Co., Urea 10E) and portable gas detector (Gastec, model 801), respectively.

## 3. Results and discussion

Conversions of NO oxidation as a function of reaction temperatures are shown in Fig. 1 with various supported catalysts. As can be seen in Fig. 1, all low Pt loaded (0.5%) catalysts exhibit appropriate conversion at 350 °C even in the absence of promoters. For the  $Pt/TiO_2$  and  $Pt/SiO_2$  catalysts, the maximum NO conversions of 45 and 43%, respectively, are obtained at 350 °C but after the addition of  $WO_3$ , the maximum

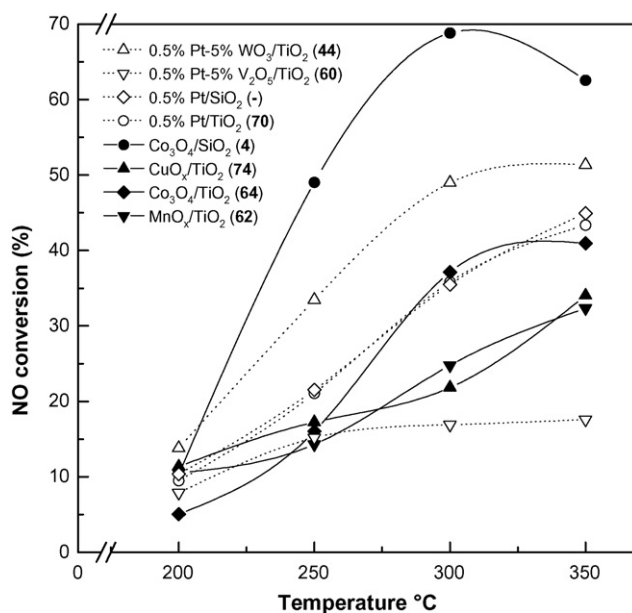


Fig. 1. Effect of reaction temperature on NO oxidation over different oxidation supported catalysts (150 ppm NO, SV = 100,000 h<sup>-1</sup>, 8% H<sub>2</sub>O, 10% O<sub>2</sub> and N<sub>2</sub> balance). Values in parenthesis show BET surface areas.

NO conversion of 51% is shifted to lower temperature to 350 °C. This is only because of the addition of electrophilic cations to the supported platinum catalysts that increases the resistance against Pt oxidation due to the increase of surface acidity. This figure also shows that the presence of  $V_2O_5$  promoter slightly suppresses the NO oxidation activity but their reaction mechanism is not clear yet [13]. However, the expensive cost of noble metals still limit the widespread application of these catalysts. Hence a number of different transition metal oxide supported catalysts have been prepared such as  $MnO_x/TiO_2$ ,  $CuO_x/TiO_2$ ,  $Co_3O_4/TiO_2$  and  $Co_3O_4/SiO_2$ . The  $MnO_x/TiO_2$ ,  $CuO_x/TiO_2$  and  $Co_3O_4/TiO_2$  do not exhibit appropriate conversion, i.e., 50% in the fast SCR process at SV of 100,000  $h^{-1}$  but in case of  $Co_3O_4/SiO_2$ , a remarkable conversion (69%) is achieved at the same SV (100,000  $h^{-1}$ ) at a lower temperature 300 °C. This shows that the support play an important role for the oxidation of NO in the fast SCR process. The sole advantage of using  $TiO_2$  and  $SiO_2$  as supports is that both of them are resistive to sulphur poisoning. Furthermore, titania support is also able to stabilize the supported oxide in highly dispersed form even at the higher metal loadings. In general, silica support affords metal oxide phases with higher crystallinity. The activities orders of these catalysts are:  $Co_3O_4/SiO_2 > Pt-WO_3/TiO_2 > Pt/TiO_2 > Pt/SiO_2 > CuO_x/TiO_2 > Co_3O_4/TiO_2 > MnO_x/TiO_2 > Pt-V_2O_5/TiO_2$ .

The activities of unsupported metal oxide catalysts for conversion of NO oxidation have also been determined as shown in Fig. 2. Among all the catalysts tested, it is clearly seen from the figure that  $Co_3O_4$  is the most active catalyst. All the catalysts exhibit more than 50% NO conversion even at 300 °C with high SV compared to the supported catalysts.  $CuO_x$  does not provide effective conversion even at higher temperature with 21% conversion at 350 °C but rest of  $Co_3O_4$  and  $MnO_x$

catalysts show 66 and 59% conversions, respectively, at 300 °C. As oxides of Co and Mn are found to be the most effective catalysts for NO oxidation hence mixed oxide of both metals have been tested for the reaction activity but it exhibits little lesser conversion (57%) from both Co and Mn oxides catalysts when they are tested separately. As  $Co_3O_4$  is very active for NO oxidation with high conversion even at lower temperatures and high SV compared with the supported and other unsupported catalysts hence this reflects  $Co_3O_4$  has more oxidizing ability [5,6]. The NO oxidation over all the developed catalysts is followed by the Eley-Rideal mechanism in which NO is in the gaseous state and oxygen is at adsorbed state as described in our previous study [14].

Since  $Co_3O_4$  catalyst is found to be the most active one among all the catalysts selected, this catalyst has been further evaluated as a function of calcination temperature, the optimum SV at 50% NO conversion into  $NO_2$  and  $SO_2$  concentrations on the NO oxidation over the supported catalysts. The effect of calcination temperature as a function of reaction temperature over  $Co_3O_4$  catalyst is shown in Fig. 3. As can be seen, at a low calcination temperature (300 °C), the activity of the catalyst becomes higher compared to the activities at higher calcination temperatures. This observation can be attributed to the decrease of surface area caused by sintering at high temperature [6]. The catalyst was calcined at 300 °C gives a maximum conversion of 76% at 300 °C with a high BET surface area (37  $m^2/g$ ) compared to the others. For instance, the catalysts were calcined above 300 °C such as 500 and 600 °C exhibits the maximum conversion of 61 and 51% at 300 °C with lesser BET surface areas of 12 and 6  $m^2/g$ , respectively. This clearly indicates that the catalyst calcined at 300 °C has the highest activity for NO oxidation. The NO conversion over  $Co_3O_4$  catalysts decreases in the order of  $Co_3O_4$  (300) >  $Co_3O_4$

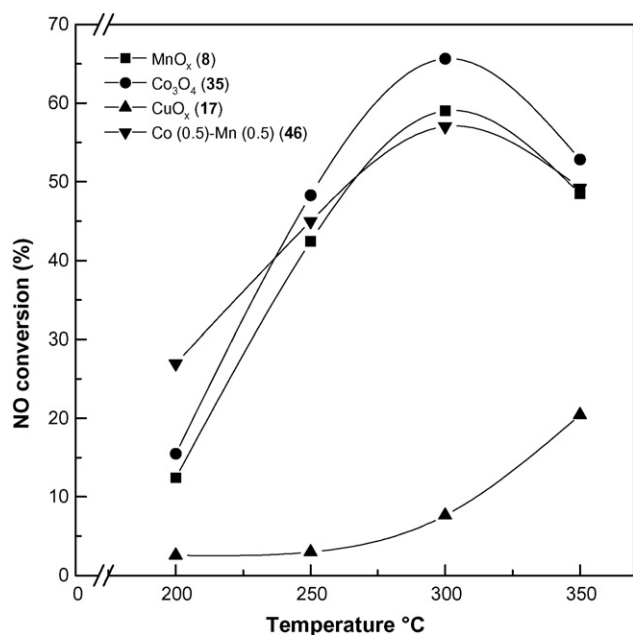


Fig. 2. Effect of reaction temperature on NO oxidation over different oxidation unsupported catalysts (150 ppm NO, SV = 150,000  $h^{-1}$ , 8%  $H_2O$ , 10%  $O_2$  and  $N_2$  balance). Values in parenthesis are BET surface areas.

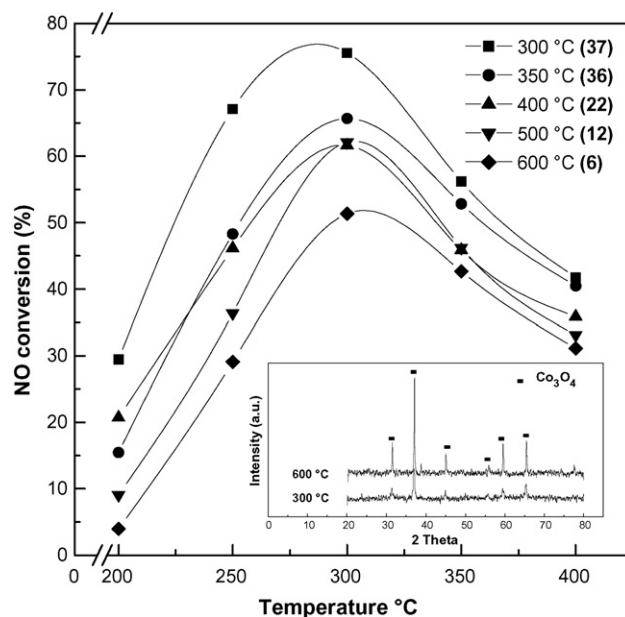


Fig. 3. Effect of calcination temperature on NO oxidation as a function of reaction temperatures over  $Co_3O_4$  catalyst; XRD analysis of  $Co_3O_4$  catalyst at different calcination temperatures (150 ppm NO, SV = 150,000  $h^{-1}$ , 8%  $H_2O$ , 10%  $O_2$  and  $N_2$  balance). Values in parenthesis are BET surface areas.

(350) >  $\text{Co}_3\text{O}_4$  (400) >  $\text{Co}_3\text{O}_4$  (500) >  $\text{Co}_3\text{O}_4$  (600) where their calcination temperatures are shown in parenthesis. In Fig. 3, the small figure shows the XRD data at lower calcination temperature of 300 °C, the peaks are broader compared with those observed at higher temperature of 600 °C where the peaks become narrow and narrow with more crystalline with increasing the calcination temperature. Thus, the catalyst was calcined at lower temperature having a smaller particle size with larger surface area and consequent increase in the conversion.

It has been reported that the reaction rate is maximum for the fast SCR process when the fraction of  $\text{NO}_2/\text{NO}_x = 0.5$ , i.e., 50% conversion of NO into  $\text{NO}_2$ . In order to achieve 50% conversion, a specific amount of catalyst has to be charged into the reactor, i.e., an optimum value of SV has to be determined to achieve 50% conversion. It is seen from Fig. 4 that at a low SV of  $150,000 \text{ h}^{-1}$ , the NO conversion is almost 77% but at a high SV of  $250,000 \text{ h}^{-1}$ , the NO conversion is almost 45% at 300 °C hence the NO conversion decreases with increasing SV. In the fast SCR process, the most efficient NO oxidation can be attained with an equimolar amount of NO/ $\text{NO}_2$ . Hence in this study, the optimum SV leading to 50% conversion at 300 °C is estimated to be  $238,000 \text{ h}^{-1}$  (0.21 g) as shown within Fig. 4.

The presence of  $\text{SO}_2$  (70 ppm) on NO oxidation with the supported/unsupported catalysts was also determined. It was found that the conversion of NO is greatly suppressed with all the catalysts tested except Pt- $\text{WO}_3/\text{TiO}_2$  that is slightly affected by  $\text{SO}_2$  as can be seen in Fig. 5 where the NO oxidation activity with all the catalysts decreases by the presence of  $\text{SO}_2$ . The formation of  $\text{NO}_2$  is shifted towards higher temperatures. The  $\text{NO}_2$  formation rate and the maximum  $\text{NO}_2$  formation are lower

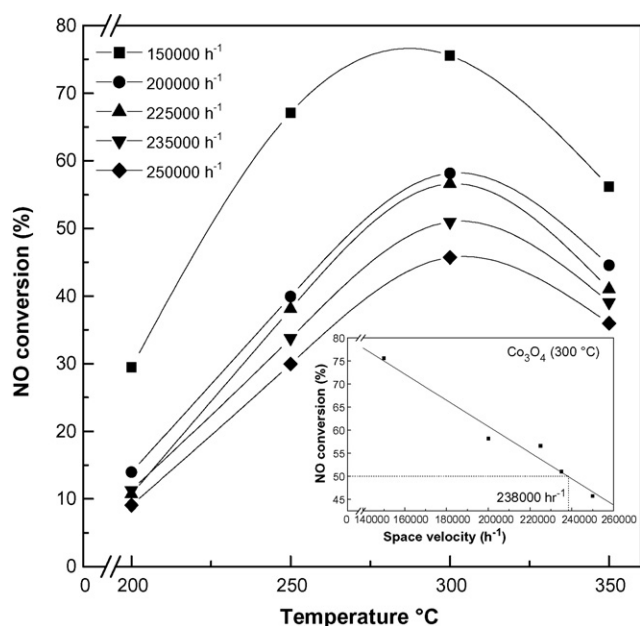


Fig. 4. Effect of reaction temperature as a function of SV on NO oxidation over  $\text{Co}_3\text{O}_4$  catalyst; small figure shows the optimum value of SV for 50% conversion of NO into  $\text{NO}_2$  over  $\text{Co}_3\text{O}_4$  catalyst at 300 °C (150 ppm NO, 8%  $\text{H}_2\text{O}$ , 10%  $\text{O}_2$  and  $\text{N}_2$  balance).

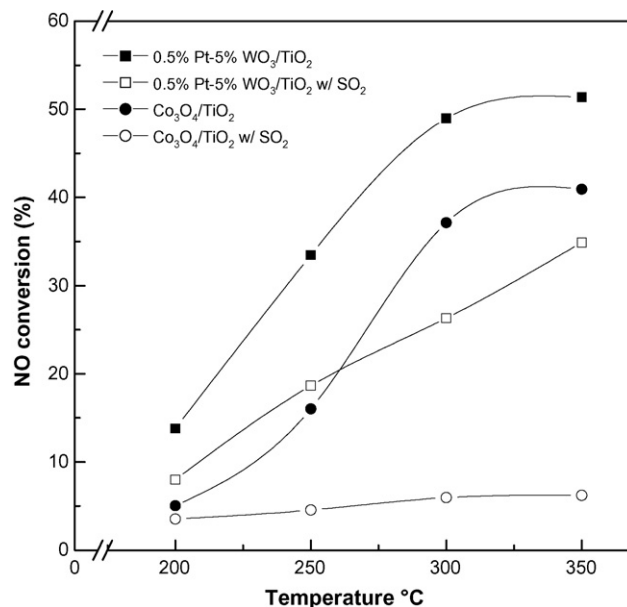


Fig. 5. Effect of reaction temperature in the presence/absence of  $\text{SO}_2$  over different  $\text{TiO}_2$  supported catalysts (150 ppm NO, 70 ppm  $\text{SO}_2$ , 8%  $\text{H}_2\text{O}$ , 10%  $\text{O}_2$  and  $\text{N}_2$  balance).

compared with the corresponding experiments in absence of  $\text{SO}_2$ . This little effect of  $\text{SO}_2$  on the Pt based catalyst is may be due to the presence of  $\text{WO}_3$ . In fact,  $\text{WO}_3$  competes with and displaces  $\text{SO}_3$  on the basic sites of  $\text{TiO}_2$  surface and tend to cover it, thus limiting its sulphation [15]. When NO and  $\text{SO}_2$  coexist in the feed,  $\text{SO}_2$  is preferentially adsorbed on the catalyst with respect to NO. Moreover, in the presence of excess oxygen,  $\text{SO}_2$  is easily oxidized to  $\text{SO}_3$  (noble metal act as catalysts for this reaction) [3] and sulphates are formed on the catalyst.  $\text{SO}_3$  can be transferred on the support surface via the spill over mechanism. When the impregnated metal reacts with  $\text{SO}_2$  to form metal sulphates, the active sites are completely covered by sulphates and as a result the catalyst is irreversibly deactivated by the presence of  $\text{SO}_2$ . Noble metals do not form sulphates but NO and  $\text{SO}_2$  oxidation takes place on these sites. The presence of sulphate species may alter the catalytic properties of the materials, causing an inhibition for the NO oxidation. In the presence of  $\text{SO}_2$ , it is clearly seen from Fig. 5 that the conversion is about 5% over  $\text{Co}_3\text{O}_4/\text{TiO}_2$  at 200 °C but the conversion is nearly 7% at 300 °C hence the activity of  $\text{Co}_3\text{O}_4/\text{TiO}_2$  is greatly suppressed by  $\text{SO}_2$ . This may also indicates that  $\text{Co}_3\text{O}_4$  is more oxidizing towards  $\text{SO}_2$  than NO as  $\text{SO}_2$  adsorbed first on the active site of the catalyst. The activity of Pt- $\text{WO}_3/\text{TiO}_2$  catalyst is also suppressed little by  $\text{SO}_2$  and the maximum conversion point is shifted to higher temperature due to formation of sulphates that are decomposed at higher temperature. As observed, over Pt- $\text{WO}_3/\text{TiO}_2$  catalyst without  $\text{SO}_2$ , the maximum conversion (53%) is obtained at 350 °C but with the addition of  $\text{SO}_2$  in the stream, the maximum conversion decreases to 35% at the same temperature. Since  $\text{Co}_3\text{O}_4$  catalyst observed to be adversely affected by  $\text{SO}_2$ ; this catalyst should be used after the desulphurization process unit.

Similar to the NO oxidation, a number of reduction catalysts (supported/unsupported) were also prepared and evaluated for



the DeNO<sub>x</sub> conversion. With all the catalysts tested, the fast SCR process gives more than 90% conversion compared to the standard SCR but the unsupported catalysts (oxides or mixed oxides) exhibit this conversion even at higher SV. Among the supported catalysts, the commercial catalyst gives the maximum conversion up to 100% at a temperature range of 250–300 °C and SV = 100,000 h<sup>-1</sup> as shown in Fig. 6(a) but, in case of the standard SCR, the commercial catalyst produces less conversion at lower temperature but at higher temperature it gives almost 90% conversion. As can be seen in Fig. 6(a), in case of the standard SCR, the conversion is almost 21% at 200 °C but it shows nearly 90% conversion at 300 °C. In case of the fast SCR, the activity order of the tested catalysts for DeNO<sub>x</sub> conversion is as follows: V<sub>2</sub>O<sub>5</sub>-WO<sub>3</sub>/TiO<sub>2</sub> > CeO<sub>2</sub>/TiO<sub>2</sub> > MnO<sub>x</sub>/TiO<sub>2</sub>. However, amongst the unsupported catalysts, the mixed oxides of Co-W Exhibit 100% conversion even at a comparatively lower temperature (200 °C) and at a higher SV (200,000 h<sup>-1</sup>). Other unsupported catalysts also exhibit the

DeNO<sub>x</sub> conversion nearly 90% in the fast SCR process even at a SV of 200,000 h<sup>-1</sup> and also these catalysts show good DeNO<sub>x</sub> conversion for the standard SCR. MnO<sub>x</sub> provides good DeNO<sub>x</sub> conversion but when this MnO<sub>x</sub> is mixed with CeO<sub>2</sub> by the PM then it gives better conversion than MnO<sub>x</sub> alone. As shown in Fig. 6(b), MnO<sub>x</sub> shows 86% conversion at 200,000 h<sup>-1</sup> in the fast SCR but after mixing with CeO<sub>2</sub> it produces nearly 90% conversion at the same SV and 300 °C. This may indicate that there is strong interaction between the manganese and cerium oxide which resulted in the high activity [6]. But among all the unsupported catalysts tested, the mixed oxide of Co-W gives the highest conversion. Since V<sub>2</sub>O<sub>5</sub> based catalyst is a commercial catalyst having its optimum at intermediate temperatures, it needs a relatively high volume for effective conversion and requires complex manufacturing method as it has a number of promoters. Hence, this study is mainly focused on the reactivity of the mixed oxide of Co-W. Co<sub>3</sub>O<sub>4</sub> has not been observed to yield satisfactory DeNO<sub>x</sub> conversion; however, after impregnation with a small amount of WO<sub>3</sub>, the DeNO<sub>x</sub> conversion with Co<sub>3</sub>O<sub>4</sub> reaches up to 100% conversion even at 200 °C in the fast SCR process. The mixed oxide of Co-W was also tested at temperature around 150 °C and it also exhibits 100% conversion but this catalyst was not found to be good in the standard SCR process as it gives almost 78% DeNO<sub>x</sub> conversion at 350 °C. Actually, in case of standard SCR, the SCR reaction proceeds according to Eley-Rideal mechanism in which ammonia first adsorbs on the active site of the catalyst and then reacts with gaseous nitrogen oxide and the reduced state of catalyst is reoxidized by oxygen but on the other hand, in the fast SCR, this reoxidizing role by oxygen is substituted by NO<sub>2</sub> that is a more effective oxidizing agent [1,16]. Moreover, the standard SCR follows the Eley-Rideal mechanism [10] but when there is NO<sub>2</sub> in the feed the mechanism changes to the Langmuir–Hinshelwood mechanism [17]. With this concept, the mixed oxide of Co-W might reoxidize the reduced state more easily or the adsorption of oxygen on this catalyst is very weak. Hence that catalyst proved to be less effective for the standard SCR than the fast SCR process. However, this excellent conversion indicates that cobalt and tungsten oxides possess strong mutual interactions and these oxides may have formed a complex species which is very active for the DeNO<sub>x</sub> conversion or they may formed some solid solution between cobalt and tungsten oxides as reported by Silva et al. [18] for the MnO<sub>x</sub> and CeO<sub>2</sub> mixed oxides. Further, Co<sub>3</sub>O<sub>4</sub> is highly active because of its high redox property and when it is combined with other oxides, the cobalt spinel catalyst shows different activities [19]. In order to see the mechanism behind the catalyst that shows its high activity, it was further analyzed by scanning electron microscopy (SEM), transmission electron microscopy (TEM) and energy dispersive X-ray (EDX) spectrometry. Fig. 7(a) exhibits high magnification SEM image of cobalt oxide nanoparticles. These rounded shaped nanoparticles or nanospheres grown in high density and agglomerated due to electrostatic force of attraction. Each nanosphere has diameter in the range of 25 ± 5 nm. The stoichiometry, pH, reaction time and temperature are responsible for precipitation of cobalt oxide nanospheres. Fig. 7(b)

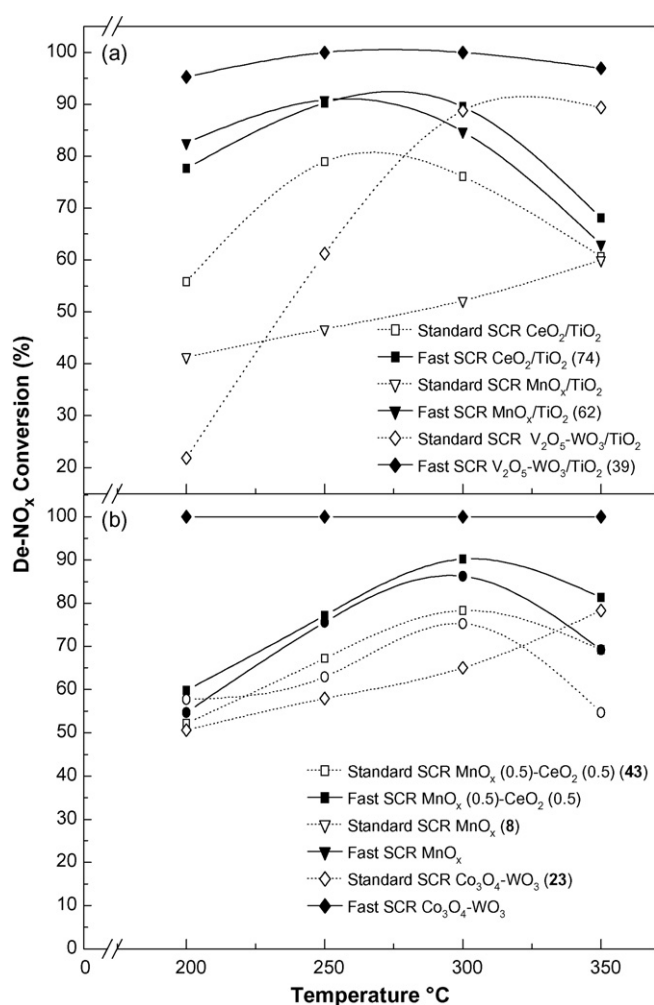


Fig. 6. (a) Effect of reaction temperature on DeNO<sub>x</sub> conversion over different supported catalysts for the standard and fast SCR processes (300 ppm NO<sub>x</sub>, NH<sub>3</sub>/NO<sub>x</sub> = 1, SV = 100,000 h<sup>-1</sup>, 8% H<sub>2</sub>O, 10% O<sub>2</sub> and N<sub>2</sub> balance). Values in parenthesis are BET surface areas. (b) The De-NO<sub>x</sub> conversion as a function of reaction temperatures over different unsupported catalysts for the standard and fast SCR processes (300 ppm NO<sub>x</sub>, NH<sub>3</sub>/NO<sub>x</sub> = 1, SV = 200,000 h<sup>-1</sup>, 8% H<sub>2</sub>O, 10% O<sub>2</sub> and N<sub>2</sub> balance). Values in parenthesis are BET surface areas.

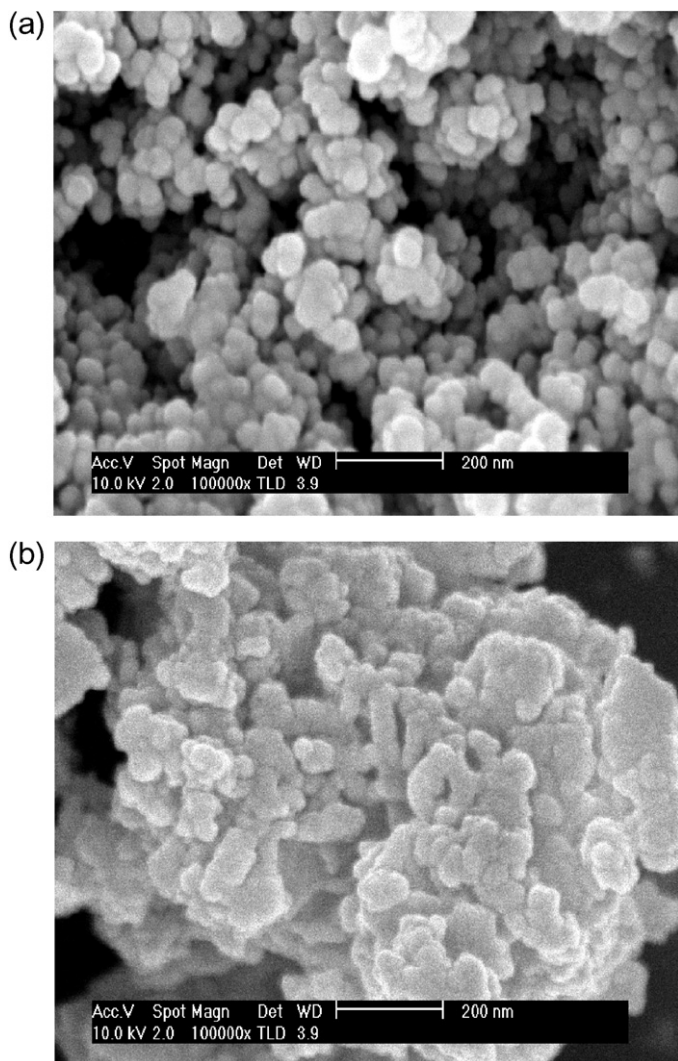


Fig. 7. (a) High magnification SEM image of cobalt oxide nanospheres. (b) High magnification SEM image of cobalt tungstate nanocomposite.

shows field emission scanning electron microscopy (FESEM) image of nanocomposite (cobalt tungstate) formed by the impregnated method. Due to impregnation morphology of the formed nanocomposite changed considerably. The regular nanospheres changed their morphology into nanocomposite crystal of cobalt tungstate (Co-W mixed oxide nanocomposite).

The chemical composition of nanospheres ( $\text{Co}_3\text{O}_4$ ) and nanocomposite of the mixed oxides (Co-W) were also analyzed by EDX spectrometry. Fig. 8(a) shows EDX spectrum of cobalt oxide. The nanospheres are formed in proper stoichiometry of cobalt, oxygen and gold. Gold peak appeared from the sample coating before FESEM measurement. Fig. 8(b) shows EDX spectrum of cobalt tungstate nanocomposite which shows an additional peak of tungsten. It was observed that the obtained nanocomposite was formed in a proper stoichiometry of cobalt oxygen and tungsten. Metal contents obtained by the EDX quantitative analysis were demonstrated in Table 1. The facile nanocomposite of (cobalt tungstate) formed by the inexpensive impregnation method, which works as novel and effective nanocatalyst to reduce  $\text{NO}_x$ .

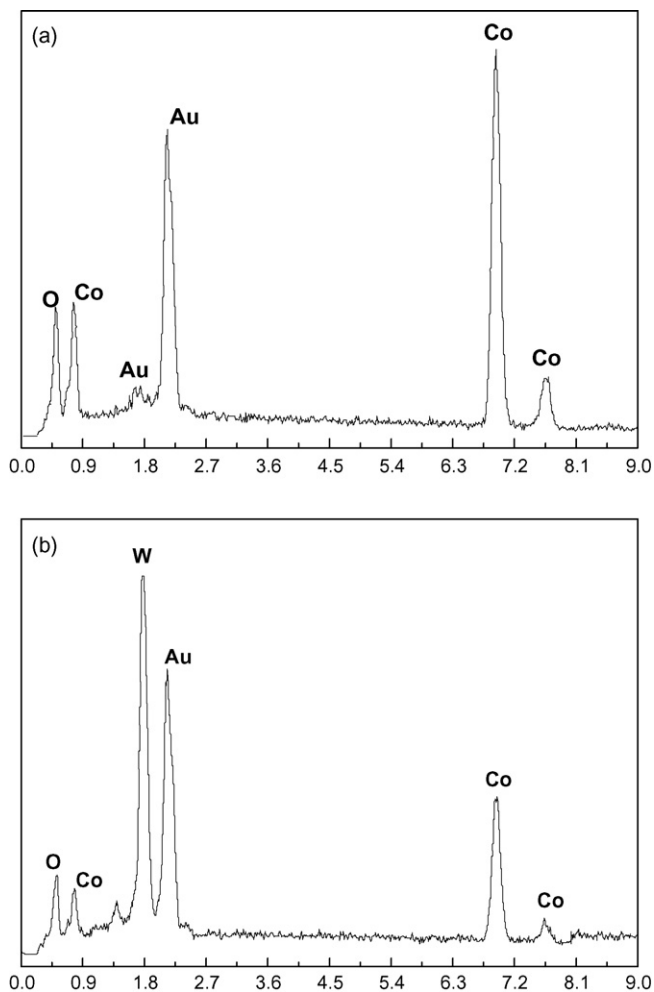


Fig. 8. EDX spectrum. (a) Cobalt oxide and (b) nanocomposite of cobalt tungstate.

Low magnification of TEM image shows the agglomerated cobalt oxide nanospheres as shown in Fig. 9(a). The magnified TEM (Fig. 9(b)) image clearly reveals that these cobalt oxide nanoparticles grown as nanospheres. The average diameter of each nanosphere is about  $25 \pm 5$  nm. The lattice fringe has its spacing of 0.472 nm, corresponding to the (1 1 1) plane as can be seen in Fig. 9(c). These results are fully consistent with the SEM results. Fig. 10(a) presents clear view of TEM image of cobalt tungstate nanocomposite that was synthesized by the simple impregnation method. Due to the impregnation, the size of nanocomposite become larger and the average diameter of nanocomposite is in the range of  $150 \pm 50$  nm. Fig. 10(b)

Table 1  
EDX quantitative analysis

Element	wt%	
	$\text{Co}_3\text{O}_4$	$\text{Co}_3\text{O}_4\text{-WO}_3$
O (K)	9.46	7.67
W (M)	–	67.04
Co (K)	90.54	25.29
Total	100	100

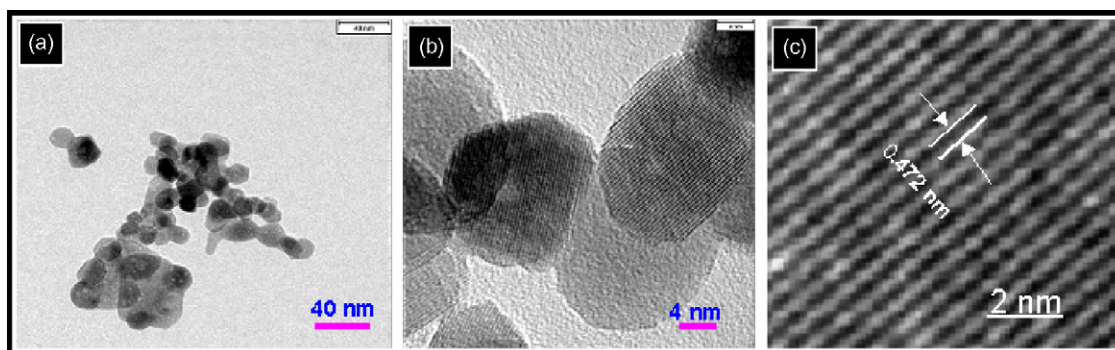


Fig. 9. (a) Low magnification TEM image, (b) high magnification TEM image and (c) HRTEM image of cobalt oxide nanospheres.

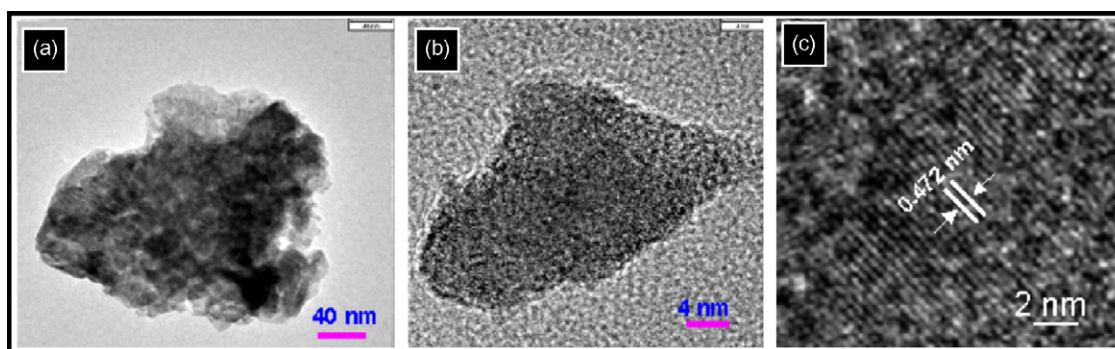


Fig. 10. (a) Low magnification TEM image, (b) high magnification TEM image and (c) HRTEM image of cobalt tungstate nanocomposite.

exhibits high magnification of TEM image of cobalt tungstate nanocomposite. It can be estimated from Fig. 10(c) that the tungstate has completely embedded on the cobalt oxide surfaces that is not observed only in the cobalt oxide sample (Fig. 9(c)). From the systematic TEM studies, the cobalt tungstate nanocomposite is proved to be formed under the mild conditions. In the cobalt oxide, the lattice fringes are very clear to be seen but not in cobalt tungstate. However, some of the lattice fringes can be observed which can be assigned to cobalt oxide only. From these analyses it can be concluded that the formation of nanocomposite takes place after the impregnation of tungsten over cobalt oxide that is highly active for the selectivity of  $\text{DeNO}_x$  conversion.

During the  $\text{DeNO}_x$  process, a specific amount of  $\text{N}_2\text{O}$  is found to be released and this amount increases with increasing temperature.  $\text{N}_2\text{O}$  can be formed by the direct oxidation of ammonia and by the reaction between ammonia and  $\text{NO}_x$ . In case of the fast SCR,  $\text{N}_2\text{O}$  formation over the mixed oxides of Co-W catalyst is found to be negligible compared to the rest of the catalysts, and found to be up to 5 ppm at 350 °C. In contrast, in the standard SCR, all the tested catalysts do produce high concentration of  $\text{N}_2\text{O}$  as shown in Fig. 11. As can be seen, in the fast SCR process with Co-W produces less than 5 ppm  $\text{N}_2\text{O}$  but the mixed oxide of Mn-Ce produces 25 ppm  $\text{N}_2\text{O}$  at 350 °C. On the other hand, in case of the standard SCR process with Co-W produces less than 38 ppm  $\text{N}_2\text{O}$  but the mixed oxide of Mn-Ce produces large amount of  $\text{N}_2\text{O}$  (92 ppm) at 350 °C. This clearly indicates that Co-W catalyst has highly reducing property and hence it prevents ammonia oxidation since  $\text{N}_2\text{O}$  is mainly

produced by this side reaction. In general, the SCR activity with pure NO increases with increasing temperature but the reaction of ammonia is also pronounced at higher temperatures. This competitive reaction between the SCR and ammonia oxidation may decrease the activity and selectivity of the reaction. Also, with increasing the  $\text{NO}_2/\text{NO}_x$  ratio up to 0.5, the amount of  $\text{N}_2\text{O}$  formation decreases but it increases with increasing the  $\text{NO}_2/\text{NO}_x$  ratio above 0.5 [20]. Since the formation of  $\text{N}_2\text{O}$  is

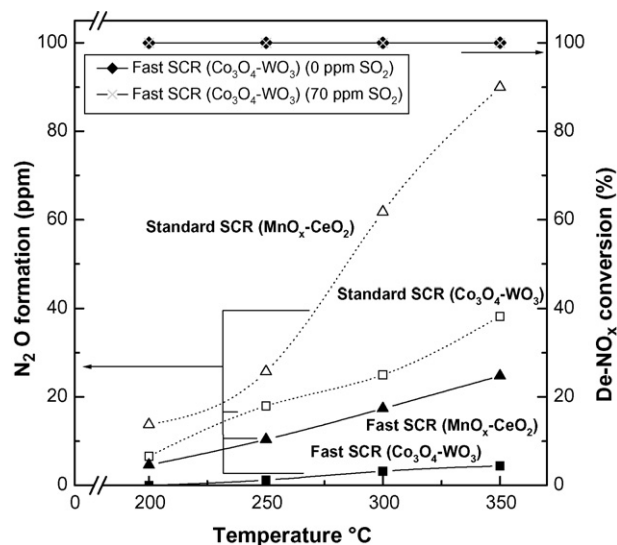


Fig. 11. Effect of temperature on  $\text{N}_2\text{O}$  formation and  $\text{De-NO}_x$  conversion as a function of  $\text{SO}_2$  over different mixed oxide catalysts (300 ppm  $\text{NO}_x$ ,  $\text{NH}_3/\text{NO}_x = 1$ ,  $\text{SV} = 200,000 \text{ h}^{-1}$ , 8%  $\text{H}_2\text{O}$ , 10%  $\text{O}_2$  and  $\text{N}_2$  balance).



comparatively smaller than the other standard and low SCR, the fast SCR reaction has better selectivity to the desired reaction than the other side reactions. The mechanism of  $N_2O$  formation by the reaction between  $NH_3$  and  $NO$  has not been fully clarified. But it was proposed that the active sites for  $N_2O$  formation and the SCR reactions are the same and suggested a nitrosamidic species as an intermediate in the formation of  $N_2O$  [21]. The SCR activity over Co-W catalyst was also tested in the dry condition and observed that the amount of  $N_2O$  formation is higher than in a humid feed condition (figure not shown) thus, water inhibits the  $N_2O$  formation [22]. The presence of water influences the decomposition of nitrosamidic species into  $N_2$ . Also shown in Fig. 11, only in case of the fast SCR, there is negligible effect of  $SO_2$  on the  $DeNO_x$  conversion over Co-W mixed oxide catalyst at temperatures below  $350^\circ C$  but the temperatures equal or greater than  $350^\circ C$ ,  $SO_2$  resulted in a slight decrease in the  $DeNO_x$  conversion. This might be attributable to the presence of  $WO_3$  that causes sulphates to become unstable at temperatures above  $350^\circ C$ . Further, it may explain that  $SO_2$  is chemisorbed on the active site of metal oxide and then forms instable sulphite ion, which react with the chemisorbed oxygen to form sulphate [23]. However,  $SO_2$  promotes the  $NO_x$  removal efficiency since the formation of surface sulphated species would increase the surface acidity [24,25] and that strong acidity favors ammonia adsorption in the SCR reaction.

#### 4. Conclusions

$Co_3O_4$  is a very effective catalyst for high conversion of  $NO$  oxidation even at lower temperature and high SV with the supported and unsupported catalysts but this catalyst proved to be less active under  $SO_2$  stream. In the presence of  $SO_2$ , the Pt based promoted catalysts should be used. At calcination temperature  $300^\circ C$ ,  $Co_3O_4$  exhibits the maximum  $NO$  conversion. The  $NO$  conversion decreases with increasing SV and the optimum SV for 50%  $NO$  conversion is found to be  $238,000\ h^{-1}$  (0.21 g). The mixed oxide of Co-W has the highest activity and yields 100%  $DeNO_x$  conversion at relatively lower temperatures and high SV due to the formation of nanocomposite after impregnation of tungsten oxide over  $Co_3O_4$ .

Moreover, the effect of  $SO_2$  on the  $DeNO_x$  conversion is almost negligible over  $Co_3O_4$  catalyst and the formation of  $N_2O$  is very low compared to other metal and mixed oxide catalysts.

#### Acknowledgement

The authors would like to thank for financial support from KESRI (R-2005-7-080), which is funded by Ministry of Commerce, Industry and Energy and partly by the Korea Research Foundation (KRF) & BK 21 project.

#### References

- [1] M. Koebel, G. Madia, F. Raimondi, A. Wokaun, *J. Catal.* 209 (2002) 159.
- [2] L. Olsson, E. Fridell, *J. Catal.* 210 (2002) 340.
- [3] E. Xue, K. Seshan, J.R.H. Ross, *Appl. Catal. B* 11 (1996) 65.
- [4] J. Despres, M. Elsener, M. Koebel, O. Krocher, B. Schnyder, A. Wokaun, *Appl. Catal. B* 50 (2004) 73.
- [5] M. Misono, Y. Hirao, C. Yokoyama, *Catal. Today* 38 (1997) 157.
- [6] G. Qi, R.T. Yang, *J. Catal.* 217 (2003) 434.
- [7] L. Singoredjo, R. Korver, F. Kapteijn, J. Moulijn, *Appl. Catal. B* 1 (1992) 297.
- [8] M. Kang, E.D. Park, J.M. Kim, J.E. Yie, *Catal. Today* 111 (2006) 236.
- [9] G. Qi, R.T. Yang, *Appl. Catal. B* 44 (2003) 217.
- [10] F. Eigenmann, M. Maciejewski, A. Baiker, *Appl. Catal. B* 62 (2006) 311.
- [11] M. Koebel, M. Elsener, M. Kleemann, *Catal. Today* 59 (2000) 335.
- [12] M. Machida, M. Uto, D. Kurogi, T. Kijima, *Chem. Mater.* 12 (2000) 3158.
- [13] J. Dawody, M. Skoglundh, E. Fridell, *J. Mol. Catal. A: Chem.* 209 (2004) 215.
- [14] M.F. Irfan, J.H. Goo, S.D. Kim, *Chemosphere* 66 (2007) 54.
- [15] R. Busca, L. Lietti, G. Ramis, F. Berti, *Appl. Catal. B* 18 (1998) 1.
- [16] G. Ramis, G. Busca, F. Bregani, P. Forzatti, *Appl. Catal.* 64 (1990) 259.
- [17] J. Blanco, P. Avila, J.L.G. Fierro, *Appl. Catal. A* 96 (1993) 331.
- [18] A.M.T. Silva, R.R.N. Marques, R.M. Quinta-Ferreira, *Appl. Catal. B* 47 (2004) 269.
- [19] L. Xue, C. Zhang, H. He, Y. Teraoka, *Appl. Catal. B* 75 (2007) 157.
- [20] J.H. Goo, M.F. Irfan, S.D. Kim, *Chemosphere* 67 (2007) 718.
- [21] N.Y. Topsoe, T. Slabæk, B.S. Clausen, T.Z. Sørensen, J.A. Dumesic, *J. Catal.* 134 (1992) 742.
- [22] G. Madia, M. Koebel, M. Elsener, A. Wokaun, *Ind. Eng. Chem. Res.* 41 (2002) 4008.
- [23] M.D. Amiridis, I.E. Wachs, G. Deo, J.M. Jehng, D.S. Kim, *J. Catal.* 161 (1996) 247.
- [24] J.P. Chen, R.T. Yang, *J. Catal.* 139 (1993) 277.
- [25] R.Q. Long, M.T. Chang, R.T. Yang, *Appl. Catal. B* 33 (2001) 97.